Comparative Constitutive Constants for Hot Working of Al-4.4Mg-0.7Mn (AA5083)

H.J. McQueen, E. Fry, and J. Belling

(Submitted 1 May 2000)

Torsion tests on as-hot-rolled Al-4.4Mg-0.7Mn alloy were conducted over the strain rate range 0.1 to 10 s^{-1} and the temperature range 200 to 450 °C. As temperature decreased and strain rate increased, the flow curves exhibited peaks that were lower and broader, followed by lower softening, and closer approach to a steady-state regime partly because fracture occurred at higher strains. In constitutive analysis, the power law was found to be inappropriate, but the exponential law was suitable. The hyperbolic sine function was found to fit more closely with stress multipliers between 0.04 and 0.06 MPa^{-1}. The activation energy was found to be 162 kJ/mol. These results were shown to be in reasonable agreement with previous studies when allowance was made for variations in composition and microstructure.

Keywords AA5083, activation energy, Al-Mg-Mn alloy, constitutive constants, flow stress, hot ductility, sinh-Arrhenius law, torsion testing

1. Introduction

Aluminum alloys with grade designation AA5083 (Table 1) have intermediate strength through solute hardening from Mg and grain refinement from Al_6 Mn particles. While they are not heat treatable, they usually derive considerable strength from substructures generated during both hot and cold forming. These processes are more difficult than in pure Al because of the solute and the dispersoids.[1–6] AA5083's annealing temperature is listed as 415 °C and its hot working range as 315 to 408 °C (solidus 574 °C). These alloys are noted for their good weldability. Their applications include welded pressure vessels; cryogenics; marine, rail, and truck transportation equipment; TV towers; and drilling rigs.[7]

The torsion testing was carried out over a range of temperature T and strain rate $\dot{\varepsilon}$, which is employed in hot rolling schedules from lay-on to finishing passes.[8–10] The flow curves were determined until fracture in order to define the onset of edge cracking as temperature declines. The starting material contained an elongated microstructure with subgrains as produced at an intermediate stage of rolling, since this was considered to be more representative of many mill stages than would a completely recrystallized starting material. It was not the objective of this paper to study as-cast properties since these rarely pose a problem because of the reasonable ductility of properly homogenized slabs at the preheat temperature.[11–13]

The constitutive equations for stress σ_p were determined in order to permit calculation of mill separating forces and torques. The analysis compared the power, exponential, and hyperbolic sine (sinh $\alpha\sigma$) functions in association with an Arrhenius T dependence.[1–5,14–17] Furthermore, the sinh function was analyzed using different values of the stress multiplier α (MPa^{-1}) in order to see the influence on the other constants in the equation.[17,18] The results are compared with those in the literature,[13,19–21] including an earlier study by one author, which had a narrower range of conditions and was dedicated primarily to microstructural observations.[22,23]

While a detailed microstructural examination was not pursued, the analysis assumes that metals may undergo both dynamic recovery (DRV) and dynamic recrystallization (DRX). Aluminum and its alloys are noted for their high level of DRV, which polygonizes the dislocation substructures to such an extent that DRX is inhibited and static recrystallization (SRX) after hot deformation is much delayed.[1–6,24–27] This is in contrast to alloys of Cu, Ni, and γ-Fe, which undergo much less DRV leading to nucleation and growth of new grains during deformation; the DRX grains develop a DRV substructure that distinguishes them from SRX grains.[3,4,24–27] Usually, Mg alloys up to 5 wt.% and above about 250 °C undergo substantial DRV so that general DRX as above is not observed.[1–6,28–33] However, in alloys containing dispersoid particles larger than 0.6 μm, nucleation is enhanced in the surrounding region as a result of the small, highly misoriented cells developed due to the accommodating, turbulent flow around the hard particles.[34,35] Such particle-enhanced DRX is only observed in Al-Mg-Mn alloys and not in Al-Mn alloys, because the DRV in the latter is high enough to reduce the strain concentration.[1–6,36–38] The DRX has been observed in extrusion,[19,20,28] compression,[37] and torsion;[22,23] however, only for conditions at 400 °C ($\leq$0.1 s^{-1}) and above ($\leq$1.0 s^{-1}).

2. Experimental Techniques

The AA5083 alloy (4.4% Mg, 0.7% Mn) was supplied by the former Comalco Rolling Mills (Sydney) and had the composition given in Table 1, which includes alloys previously studied.[15,19–23,39,40] The 18 mm thick plate had been reduced 95.5% from 470 mm DC cast ingot and was used without any additional heat treatment. The specimens with axes parallel to the rolling direction were machined to the following dimensions: gauge

H.J. McQueen, E. Fry, and **J. Belling,** Department of Mechanical Engineering, Concordia University, Montreal, PQ, Canada H3G 1M8. Contact e-mail: mcqueen@vax2.concordia.ca.

Table 1 Compositions

	Mg	Mn	Cr	Fe	Si
Specifications[7]	4.0 to 4.9	0.4 to 1.0	0.05 to 0.25	0.40 max	0.4 to 0.7
Present	4.4	0.7	…	…	…
5083[22]	4.45	0.74	0.09	0.3	0.14
5083[21]	5.24	0.64	0.07	0.22	0.12
	4.47	0.73	0.14	0.23	0.13
	4.39	0.84	0.14	0.24	0.08
5083[15,29]	4.55	0.7	0.17	0.17	0.05
5456[19]	5.1	0.7	0.12	0.18	0.06
5182[18]	4.5	0.35	…	…	…
5182[43]	4.66	0.31	…	0.21	0.06
5052[43]	2.41	0.07	0.17	0.27	0.11

length 20 mm and radius 3.35 mm with shoulders having length 54 mm, radius 7 mm, and threaded grips.

The specimens were deformed in the hot torsion machine at the Melbourne Research Laboratories of BHP (Steel) Proprietary. This machine was essentially a lathe with mechanically variable speed and a heavy fly wheel, which was brought to the correct angular velocity before testing.[41] Under command from a computer, a fast-acting magnetic clutch was engaged and disengaged at a selected strain or when the stress dropped at fracture. The torque was measured by a load cell on the tail stock, which could slide along the lathe bed. Tests were conducted at strain rates of 0.1, 1.0, and 10 s^{-1} and temperatures of 200, 250, 300, 400, and 450 °C.

The specimens were secured into gripping bars, which were free to displace in chucks well outside the furnace. The specimen was enclosed in a refractory glass tube through which argon flowed during the test. The specimens were heated to temperature in 2 min by a radiant furnace controlled automatically. The temperature was measured by thermocouples in axial holes drilled into both shoulders; the one at the fixed end was used for control throughout the test. The furnace was moved along the specimen until the two ends were balanced; the temperature gradient from either shoulder to center was less than 5 °C (as determined previously by a gauge mounted thermocouple). After about 5 min, the gripping bars were locked into the chucks (so there could be no longitudinal compression and buckling during heat up). The torque Γ was recorded digitally and printed out as a function of number of rotations N. From these, equivalent stress σ and equivalent strain ε were calculated according to the von Mises criterion:

$$\sigma = (\sqrt{3}/2)\pi r^3 (3 + m'' + n'') \qquad \text{(Eq 1)}$$

$$\varepsilon = (2\pi N/\sqrt{3})(r/L) \qquad \text{(Eq 2)}$$

The strain rate sensitivity m'' ($=d\sigma/d\dot{\varepsilon}$ is determined from plots of log Γ versus log $\dot{\varepsilon}$. The work-hardening rate n'' ($=d\sigma/d\varepsilon$) is taken as zero at the steady state or peak stress.[16,22,23]

Upon fracture of the specimen, the fixed end was rapidly withdrawn from the furnace and the protective tube was removed automatically. The specimen was automatically stopped in a chamber where it was quenched by water sprays. The quenched end was observed by optical microscopy to determine the retained hot-worked structure, whereas the rotation end, which was cooled in approximately 5 min, was inspected for possible static microstructural changes.

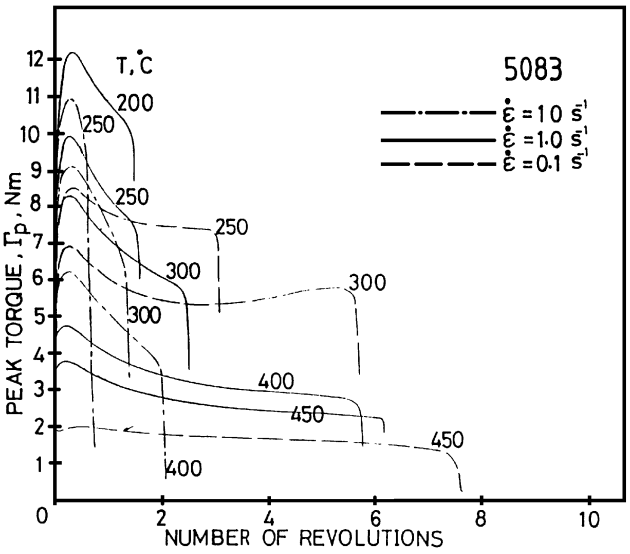

Fig. 1 Representative torque-twist curves for as-rolled 5083. The set at 1.0 s^{-1} clearly shows the decrease in peak stress, increase in ductility, and the closer approach to steady state as T rises. A few curves at 0.1 and 1.0 s^{-1} show that σ_p increases and $\dot{\varepsilon}_f$ decreases as $\dot{\varepsilon}$ rises

3. Results

Representative torque-twist curves are presented in Fig. 1. Emphasis is placed on the maximum values Γ_p; the decline is probably due to deformation heating below 400 °C and possibly to DRX above 400 °C.[22,23] At 1.0 s^{-1}, it can be seen that the torque diminishes from 12 Nm at 200 °C to 3.7 Nm at 450 °C. At 250 °C, Γ declines from 11 Nm at 10 s^{-1} to 8.5 Nm at 0.1 s^{-1}, whereas at 450 °C, the decline is from 5.2 to 2.0 Nm. Moreover, from the curves, it can be appreciated that the fracture strain $\dot{\varepsilon}_f$ increases from 250 to 450 °C: 0.8 to 2.6 turns at 10 s^{-1}, 1.7 to 6.1 turns at 1.0 s^{-1}, and 3.1 to 7.6 turns at 0.1 s^{-1} (1 turn $\approx$ 0.5). At 10 s^{-1}, for all T, and at 0.1 s^{-1}, below 300 °C, the steep declines are terminated by failure before there is any approach to a steady-state regime. The peak revolution rises from 0.1 to 0.4 as T drops at 1.0 s^{-1}; however, at 0.1 s^{-1}, they are not significantly less, and at 10 s^{-1}, they are only slightly larger. At 10 s^{-1} and 250 °C, cracking may have lowered the peak values. At 1 s^{-1} and 300 °C, one can only surmise that the slight final rise is due to a decline in temperature related to thermocouple error.

In order to calculate the stress by means of Eq 1, the values of m are obtained from plots of log Γ versus log $\dot{\varepsilon}$ (Fig. 2) and are found to decrease with falling T: 450 °C, 0.207; 400 °C, 0.136; 300 °C, 0.0644; and 250 °C, 0.0544. Consequently, σ_p is increased by about 7% at 450 °C compared to Γ_p. When σ_p is plotted against T (Fig. 3a), they decline in smooth curves with the rate of decline diminishing as T rises.[16,22,23] The three strain rates are almost parallel. When σ_p is plotted against $\dot{\varepsilon}$ (Fig. 3b), the climb from 0.1 to 1.0 s^{-1} is fairly steep but the slow rise to 10 s^{-1} indicates a saturation.

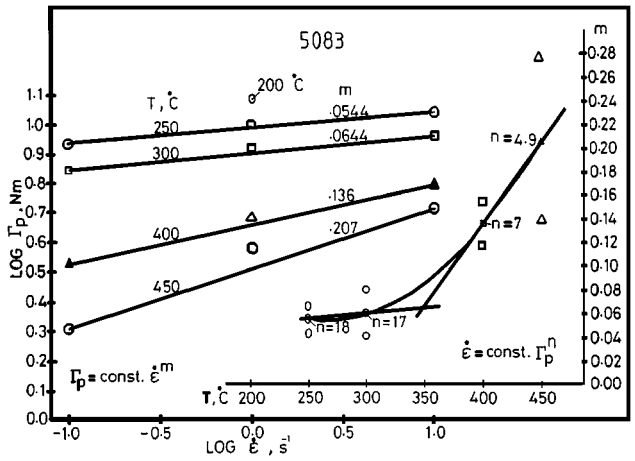

Fig. 2 This double logarithmic plot of torque against strain rate for determining precisely how the strain rate sensitivity increases as T rises. The insert (b) shows that m rises rapidly above 350 °C; the stress exponent n varies inversely

The data were fitted to the following three constitutive equations:[15,16,18,21,22,40]

$$A_p\sigma^{np} = \dot{\varepsilon} \exp (Q^P_{HW}/RT) = Z_P \qquad \text{(Eq 3)}$$

$$A_E \exp (\beta\sigma) = \dot{\varepsilon} \exp (Q^E_{HW}/RT) = Z_E \qquad \text{(Eq 4)}$$

$$A_S (\sinh \alpha\sigma)^n = \dot{\varepsilon} \exp (Q^s_{HW}/RT) = Z_s \qquad \text{(Eq 5)}$$

where A_P, A_E, A_S, n_p, n, β, α, and R (8.31 J/mol K) are constants, and Q^P_{HW}, Q^E_{HW}, and Q^S_{HW} are activation energies. The Zener-Hollomon parameter Z is a T compensated $\dot{\varepsilon}$. In the power-law plot (Eq 3), the slopes of constant T lines increase from 4.9 at 450 °C, to 7 at 400 °C, to 16 at 300 °C, and to 18 at 250 °C (Fig. 4). Such n_p values ($1/m = n_p$), which are consistent with those in Fig. 2, indicate a very slow rise up to 350 °C.

In fitting to the exponential law (Eq 4), log $\dot{\varepsilon}$ versus σ provides a series of straight lines that are almost parallel (Fig. 5). The values of β range through 0.062 MPa^{-1} (450 °C), 0.069 (400 °C), 0.095 (300 °C), and 0.089 (250 °C), giving an average value of 0.08. The higher slope at the lower temperatures is probably the result of deformation heating at 10 s^{-1}. This function gives a relatively good fit to the data, and since there is no multiplier to σ on the natural scale, it makes comparison of raw data from other sources much simpler as will be realized in the discussion.[15,21,22] Mathematical analyses of Eq 4 and 5 show that β should be approximately equal to αn, which is illustrated in the analysis of Eq 5 to follow. The activation energy is 145 kJ/mol.

In the sinh $\alpha\sigma$ analysis, the value of α is often taken from similar alloys, as found in the literature.[15,16,22,42–44] This has the advantage of facilitating comparison of data graphically and of the derived values of Q_{HW} and n. In theory, the value of α should be selected to bring the constant T lines into parallelicity. If this is done by simple graphical techniques, possibly in conjunction with a published α, there is an indeterminate error; manual methods of finding the optimum α can be time consuming. Computational programs that attempt to optimize all the coefficients are complex; moreover, they may assign different values of α to similar alloys, which makes comparison of n and Q_{HW}[15,19,20] difficult. In this analysis, it was decided to vary α from 0.01 to 0.67 MPa^{-1} to see how the other coefficients varied and the extent of the error. This is part of a long-range plan to find a universal value of α for commercial Al alloys.[16,17]

Plots of log $\dot{\varepsilon}$ versus log sinh $\alpha\sigma$ and log sinh $\alpha\sigma$ versus $(1/T)$ for α of 0.04 and 0.06 MPa^{-1} are given in Fig. 6(a) and (b), respectively. For each set of constant T data, as in Fig. 6(a), the least-squares fit is calculated, giving a value of n; the average value of n is calculated for each value of α selected; the $n_{\alpha v}$ values are listed in Table 2. For each set of constant $\dot{\varepsilon}$ data in the Arrhenius plots, as in Fig. 6(b), the least-squares

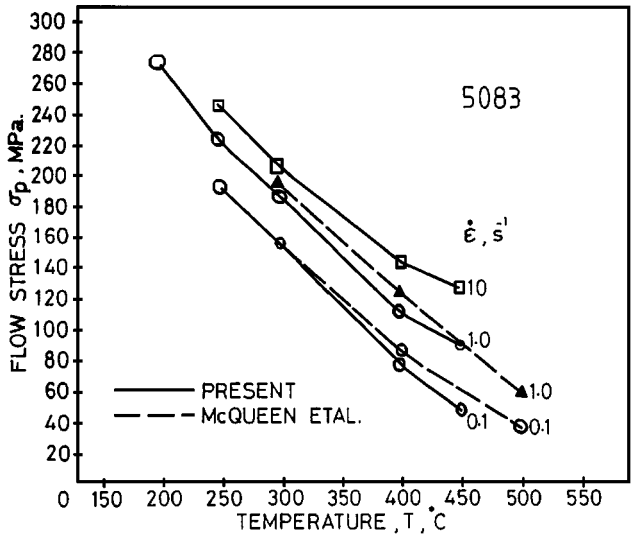

(**a**)

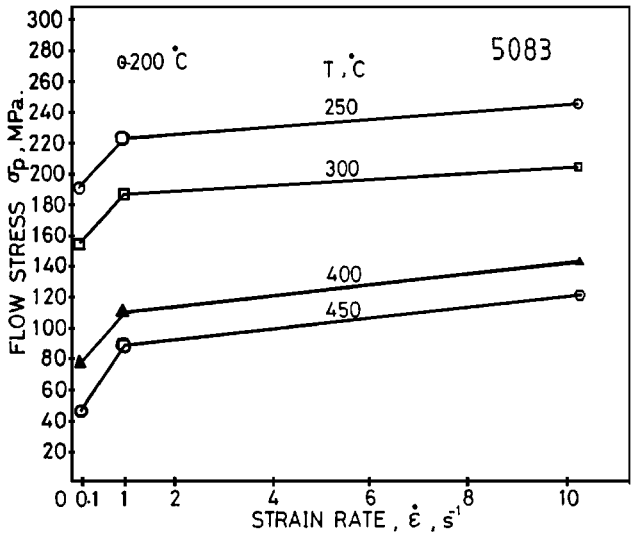

(**b**)

Fig. 3 The flow stress decreases (**a**) smoothly at a diminishing rate as T rises. The data of McQueen *et al.*[22] are in reasonable agreement. The stress rises rapidly (**b**) between 0.1 and 1 s^{-1} but slowly from 1 to 10 s^{-1}

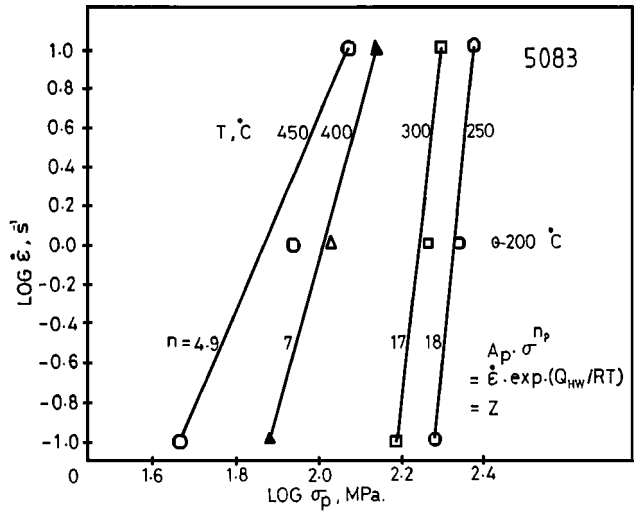

Fig. 4 The plot of log $\dot{\varepsilon}$ vs log σ_p shows that the slope n in the power law (Eq 3) rises rapidly as T falls, indicating power-law breakdown. The n values = (1/m) are in agreement with the m values in Fig. 2

line and slope S are calculated; the average value of S for each α is calculated. Plots of n versus α in Fig. 7(a) show that n declines with decreasing variation toward saturation at about 1.0 as α increases. For higher T, n is lower, as in the power law, notably at $\alpha = 0.01$ MPa^{-1}. Similar plots of S versus α in Fig. 7(b) show that the S increases almost linearly as α rises, but with slightly increasing variation being lower for higher $\dot{\varepsilon}$. From the values of n and S, Q_{HW} is calculated from

$$Q_{HW} = 2.3\, n\, RS \qquad \text{(Eq 6)}$$

The values are calculated with average S but individual values of n for each T (Fig. 7c). They are also calculated with average n but individual values of S for each $\dot{\varepsilon}$. When plotted against α, Q_{HW} is divergent for α less than 0.03 MPa^{-1} but is stable between 0.04 and 0.06 and MPa^{-1}. The average Q_{HW} is 162 kJ/mol in this range, being slightly lower when α is below 0.03 MPa^{-1}.

To obtain average $n = 5$, as in the power-law ideal for pure metal creep, $\alpha = 0.0141$ MPa^{-1} in a domain where n and, consequently, Q_{HW} are quite divergent for different T and $\dot{\varepsilon}$. It thus appears α values of 0.04 and 0.06 MPa^{-1} are suitable, because n is almost saturated with low divergence and Q is stable; however, S is rising linearly as in most of the α range and is becoming slightly more divergent. The values of $\alpha n = \beta$ are indicated in Fig. 7(a), and the average value from Fig. 5 falls near $\alpha = 0.05$ MPa^{-1}. The final step in the analysis is to derive A, which is done by calculating Z for each condition for selected values of α. The plots in Fig. 8 show that there are good fits for 0.04 MPa^{-1} (correlation coefficient 0.99718) and for 0.06 MPa^{-1} (0.99724), but a poorer fit for 0.01414 MPa^{-1}. The slope of each line gives a value of n almost identical to the average n. The intercepts of the lines give the values of A. All the constitutive constants are listed in Table 2.[15,16,20–22,39,40,42–44]

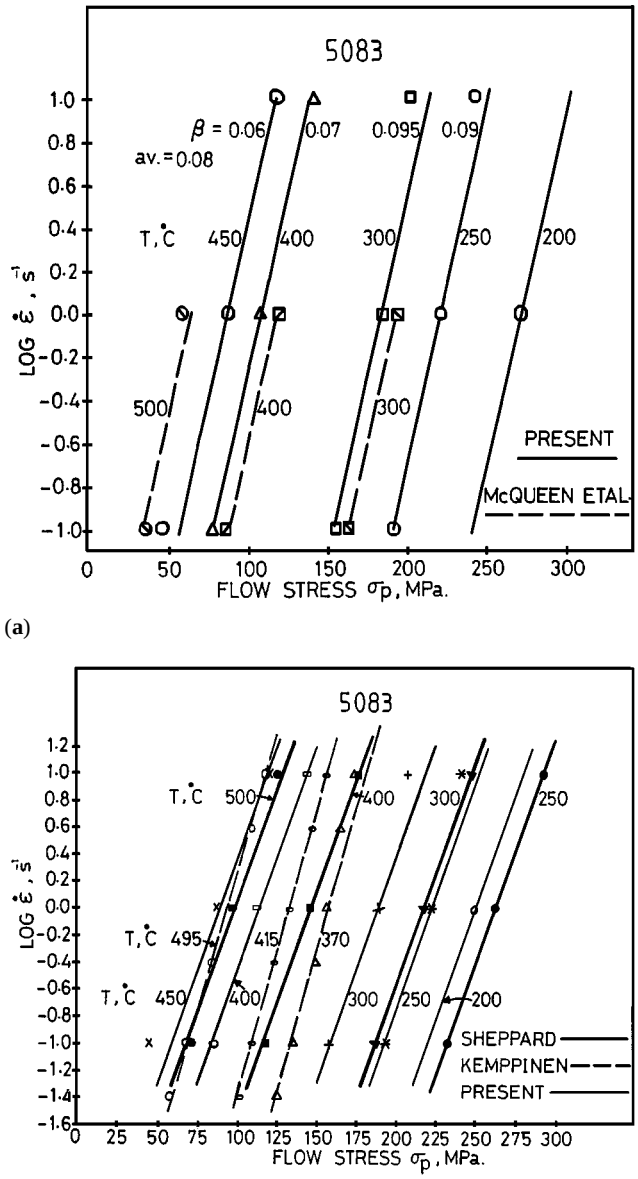

Fig. 5 The exponential law (Eq 5) proves to be a good representation of the $\dot{\varepsilon}$ dependence of σ_p. The slopes for the best-fit lines are 0.09, 0.095, 0.07, and 0.06 MPa^{-1} as T rises through 250, 300, 400, and 450 °C, respectively; the lines are drawn at average slope $\beta = 0.08$ MPa^{-1}. Data from various sources are shown in (**a**) and (**b**) for comparison[14,15,19–22]

4. Discussion

In the flow curves of 5083, the peak and work softening toward a steady-state regime are both more marked and broader than in Al-5Mg[45–47] and are considered indicative of DRX, although they may result from other morphological changes or from deformational heating. Microstructural studies by McQueen and co-workers[22,23] and by Sheppard *et al.*[19,20,28] showed that, for $\dot{\varepsilon} \leq 0.1$ s^{-1} at 400 °C and at higher T, DRX occurred. This was shown to be the result of nucleation enhancement at Al_6Mn particles larger than ~2 μm, even though fine

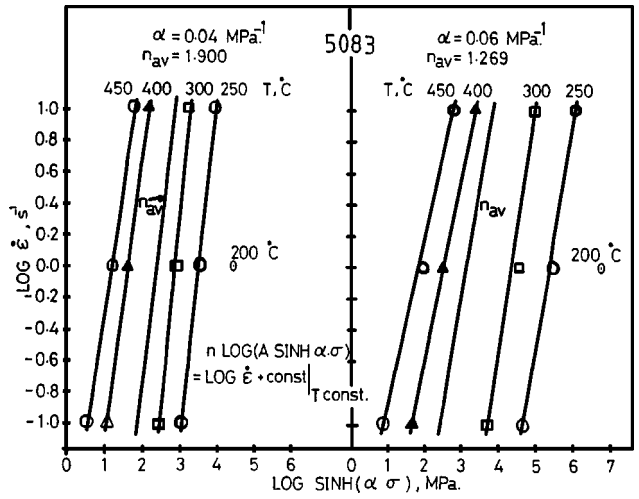

(**a**)

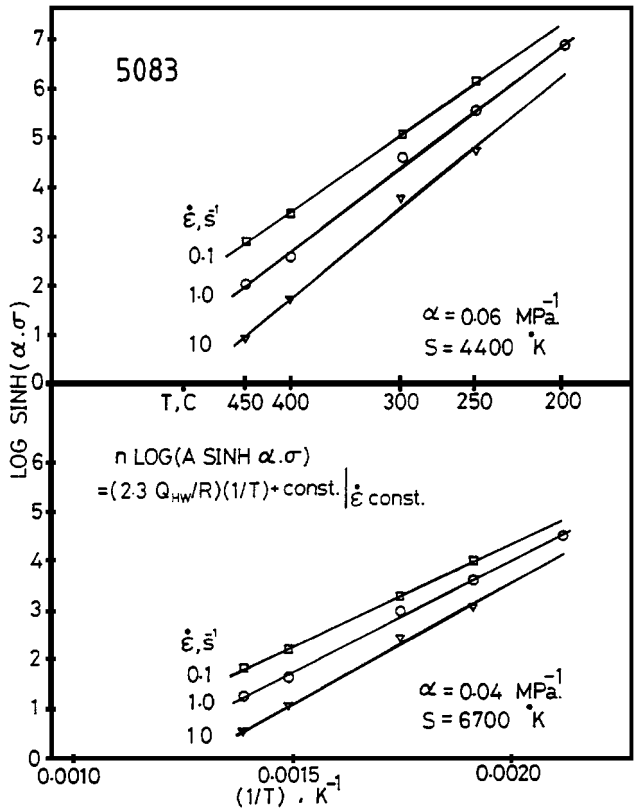

(**b**)

Fig. 6 The analysis according to Eq 5 in a log $\dot{\varepsilon}$ vs log sinh $\alpha\sigma$ graph (**a**) includes lines for $\alpha = 0.04$ and 0.06 MPa^{-1}. The associated Arrhenius relationship is shown for the two values of α (**b**). The slopes n in (**a**) and S in (**b**) are used to calculate Q_{HW} by means of Eq 6

Al_6Mn particles stabilized the substructure and limited the growth of the new grains.[3,4,19,20,32–37,45,46] Further research showed that DRX takes place in the Mn-bearing alloys when the Mg content is not less than 4% (except when the fine particles are coalesced)[34,36,37] and that DRX is sped up when the Mg content rises to 7 or 8%.[28] The absence of rising peak strain with decreasing T and rising $\dot{\varepsilon}$ may arise from the presence of the as-rolled substructure, which should make DRX somewhat easier under any condition. Rolling with limited pass strains and intervals showed some PSN-SRX nuclei in TEM.[29] In a recent study, Blum and co-workers[45–48] observed geometric DRX on Al-4.9Mg-O.6Mn, which may be an alternative explanation to particle stimulated nucleation (PSN)-DRX.

The ductility increases with rising T (fracture strains for l s^{-1}: 2.1, 3.1, 7.0, and 7.5 at 250, 300, 400, and 450 °C) and decreases with rising $\dot{\varepsilon}$ (for 400 °C: 2.6, 7.0, and 9.0 at 10, 1.0, 0.1 s^{-1}). These torsional ductilities are slightly less than those of Al-5Mg[39] and 5182[49] but only one quarter that of Al-2Mg and one eighth that of Al.[39] This is in agreement with failure by grain boundary (GB) cracking, which is common at high T. Stress concentrations from differential GB sliding are relaxed more at lower Z, diminishing initiation and propagation of GB fissures.[1,4,16,24,25,39,40] The variation with $\dot{\varepsilon}$ is in contrast with results at much lower $\dot{\varepsilon}$, where increasing decreases the relative proportions of GB sliding to lattice strain, raising ductility. In addition to cavitation at GB junctions, there is pore initiation at constituent particles.[50,51] Elongations of about 125% have been attained at 450 °C, but failure occurred by shear linking of the voids.[21,51,52] Ductility rose with increasing m value but decreased with rising particle content so that elongations of 5083 (4.46Mg-0.84Mn) remained similar to alloys with a lower Mg and Mn content of 5052 (2.34Mg-0.06Mn) or 5154 (3.31Mg-0.04Mn).[21,52,53] Low ductilities, which are associated with more severe edge cracking, have also been related to as-cast dendritic segregation and particles.[52] The GB sliding can be changed from deleterious to advantageous in 5083 by refining the grain size through heavy straining and particle-enhanced recrystallization.[1,51,52,54] Such very fine grains are capable of superplastic deformation (300 to 400%) at about 10^{-4} s^{-1} but are still prone to pore formation, particularly at hard particles.[1,51,52,55]

In the past, comparisons were made between published results on the basis of values of n and Q_{HW}. This is somewhat unsatisfactory if the constitutive equation has a different form[16–18,21,40,42,43] or even a different value of α in the sinh analysis.[15,16,20,22,39,42] For this reason, it was decided to make the substantial comparison through the sinh analysis with $\alpha = 0.04$ MPa^{-1}. The results in a parallel study on 5182 (4.5Mg-0.35Mn) gave good agreement with the present study only after some corrections (Table 2), which are explained elsewhere.[18] The torsion results of McQueen and co-workers[22,23] were originally reported for $\alpha = 0.045$ MPa^{-1} (0.067 ksi^{-1}, incorrectly stated as MPa^{-1}) with values of $n = 1.67$ and $Q_{HW} = 164$ kJ/mol. For the present alloy at the same α, $n = 1.69$ and $Q_{HW} = 162$ kJ/mol, which is very good agreement. However, when the actual stress values are entered into Fig. 5, they appear to be about 10% higher, although they follow the same trends. On recalculation for $\alpha = 0.04$ MPa^{-1}, it was determined that $n = 1.73$ and $Q = 156$ kJ/mol compared to the present 1.90 and 162 kJ/mol (Table 2), which shows that the variation with α is not identical. When the data are plotted as log Z vs log sinh $\alpha\sigma$ (Fig. 9), the lines are almost parallel to the present results but at a higher stress consistent with the higher levels of Mg and Mn (Table 1). Microstructural examination by McQueen and co-workers[22,23] showed that such constitutive

Table 2 Constitutive constants

Alloy	Mode	σ MPa^{-1}	n	Q kJ/mol	A 10^{-9}s^{-1}	ln A	Reference
5083	TOR	0.014	5.00	160.3	7.0		Present
		0.015	4.76	160.4			Present
		0.040	1.90	162.2	3.5		Present
		0.045	1.69	162.3	3.0		Present
		0.060	1.27	162.3	2.2		Present
		0.067	1.14	162.3	2.1		Present
	(exponential β = 0.08)			145			
	(power)		4.9			450; 400 °C	
5083	TOR	0.045	1.67	164			McQueen and co-workers[22,23]
		0.067					
		0.040	1.73	155.8	1.152	20.86	recalculated
5083	TEN			178			Kempinnen[21]
		0.040	2.26	185.4	3.526	21.98	recalculated
5356	(exponential β = 0.058)		179				
5083	TOR	0.015	4.99	171.4		23.11	Sheppard[15]
		0.040	1.82	162.5	0.287	19.48	recalculated
5456	TOR	0.019	3.2	161.2		23.55	Sheppard[19]
5182	TOR	0.040	2.7	218			Belling and McQueen corrected[18,49]
		0.040	2.3	185			
		0.040	2.0	174		400–500 °C	
5182	TOR	(β = 0.90)		145			Pickens and co-workers[11,12]
5182	TOR	0.062	1.35	174.2		22.48	Sheppard[15]
		0.040	2.1	177.5	0.327	19.61	recalculated
5182	COMP	0.025.78	196	264			Wells[43]
5052	COMP	0.027.11	196	1460			Wells[43]
Al-5Mg	TOR	(power)	4.8	160			Ueki *et al.*[40]
Al-5Mg	TOR	0.043		198			Cotner and Tegart[39]
Al-		(review)	0.043	4.0	156		Wong and Jonas[42]

behavior was associated with DRV below 400 °C but particle-enhanced DRX above that.

The results of tensile tests by Kempinnen[21] were presented in a power-law analysis with significant scatter. From the graph, the best average stress values were estimated at four temperatures and six strain rates. When subjected to sinh analysis at α = 0.04 MPa^{-1}, the constitutive constants were 2.26 and 185 kJ/mol, both of which are considerably higher than the present values. For 5356 (4.7Mg-0.1Mn-0.08Cr), an exponential analysis gave β = 0.058 and Q_{HW} = 179 kJ/mol.[21] In Fig. 5(b), the magnitudes of σ are seen to be higher than the present ones. In Fig. 9, the slope is higher, indicating that σ does not increase as much at high Z possibly because of necking at lower strains. The higher Q is the result of the higher n, that is, lower m, also related to necking. Tensile tests on 5083 were also conducted by Lloyd,[53] who showed that the yield stress decreased as T rose, as in Fig. 3; these values show the same trend but are very low since $\dot{\varepsilon}$ Å 10^{-3} s^{-1}. The m values were higher than in torsion, but they exhibited a similar rapid rise starting at 300 °C, instead of 350 °C. Because coarse-grained 5083 exhibits limited m values, it has limited ductility compared with dispersoid-free Al-5Mg in which consistently high m (>0.35) gives rise to high ductilities (>300%).[1,6,56]

As a result of a computer program that optimized all the constants, Sheppard published the following values for AA5083: α = 0.015 MPa^{-1}, n = 4.99, Q = 171 kJ/mol, and ln A = 23.11.[15] The coupled α and n values are consistent with the present derivation for the creep ideal. From the above coefficients, a set of peak stresses were generated for the experimental conditions employed presently; this was done since such data were not included in the publication. These are shown in Fig. 5(b) and in Fig. 9, where they are seen following the same trend but to be about 40% higher than the present results; the difference is probably due to composition but cannot be verified since it was not reported. When the constants are calculated from the data set for α = 0.04 MPa^{-1}, the values are n = 1.82 and Q = 162.5 kJ/mol, which are remarkably consistent with the present ones. For 5456 (5.1Mg, 0.7Mn), the constitutive constants were found to be α = 0.019 MPa^{-1}, n = 3.2, and Q_{HW} = 161 kJ/mol, which are in reasonable agreement with the other results discussed above.[19,20] For this alloy, Sheppard and co-workers[15,20,28,31,57,58] and Humphreys and Kalu[36] showed in both torsion and extrusion for the present $\dot{\varepsilon}$ and T ranges that DRX occurs due to particle-enhanced nucleation, but it does not occur in Al-5Mg; moreover, DRX proceeds more readily in alloys with 7% Mg.[15,57,59]

The flow stresses of 5083, measured in torsional multistage tests by Ueki *et al.*,[13,40] are presented in Fig. 5(a). The strengths of material homogenized for either 24 h or for 4 h are about 20% different, as indicated by the low and high ends of the bars. The low stress levels and rates of increase with rising $\dot{\varepsilon}$ or falling T possibly arise from the carryover of a coarser softer substructure from the preceding stages,[4,8,9,24] in contrast to the constant substructure employed here. The power law was used to fit data from torsion tests of Al-5Mg, the constants being n = 4.8 and Q_{HW} = 160 kJ/mol (Table 2).[40] Analysis of the torsion tests of Cotner and Tegart indicates that Q_{HW} for 5% Mg is 160 kJ/mol (Table 2).[16,39] Torsion tests on 5182 exhibited strengths only slightly less than 5083 but Q_{HW} of 174 kJ/mol after correction.[18,49]

The consistency in constitutive behavior between the present

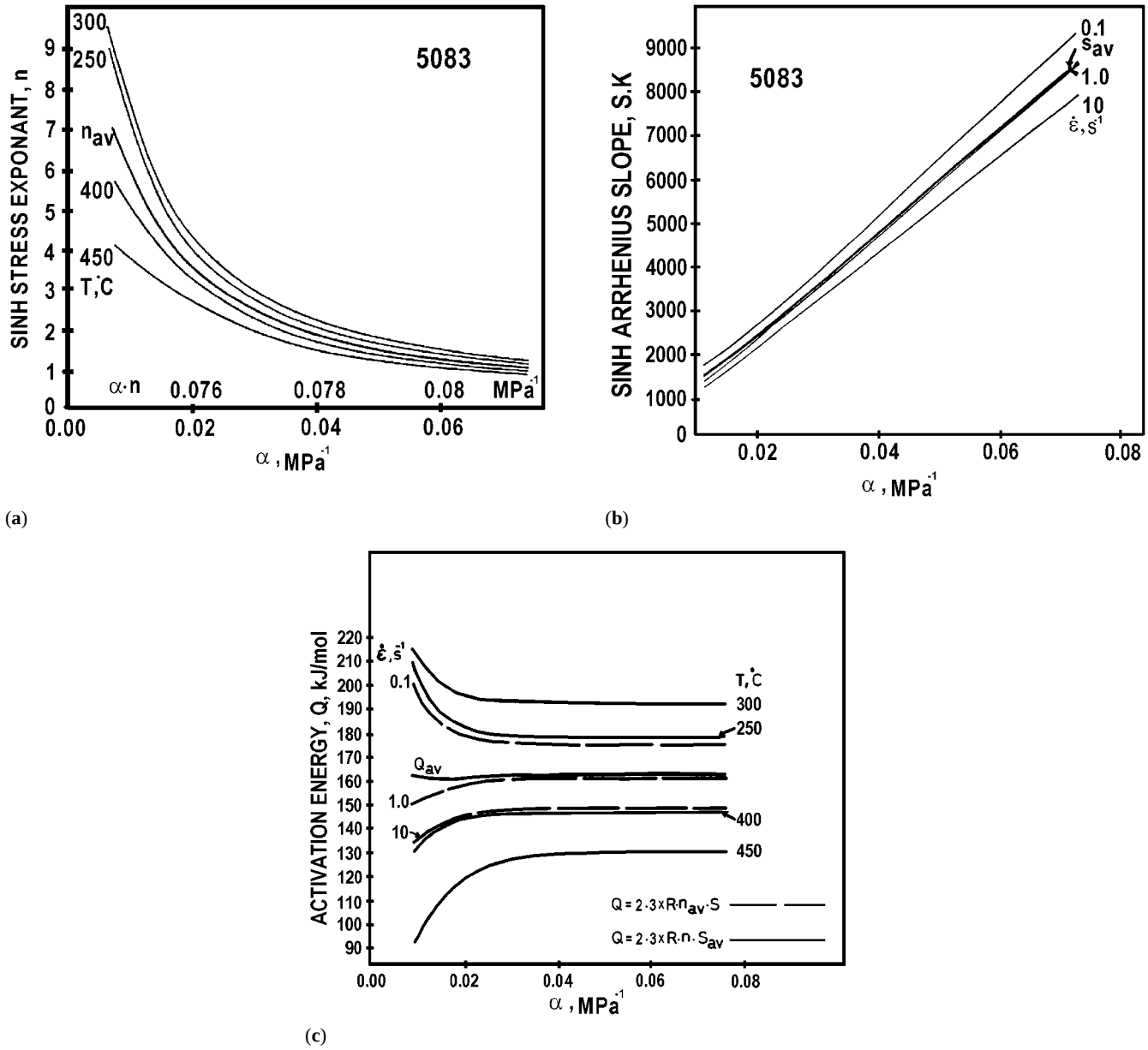

Fig. 7 The average values of n for each T grow closer together and decrease toward saturation as α increases (**a**). The average value of S for each $\dot{\varepsilon}$ increases almost linearly and with a slight divergence as α rises. The activation energies Q from the products of the various n and S values appear (**c**) to be almost constant from 0.07 down to 0.03 MPa^{-1}, where they diverge rapidly although the average is almost constant

results and the previous ones is remarkable. This can be confirmed from Fig. 9, in which the present line lies below that of Kempinnen[21] and above those of McQueen and co-workers[22,23] and of Sheppard.[15] In absolute magnitude of the present values at about 400 °C and 1.0 s^{-1} (Fig. 5), the strength of McQueen and co-workers[22,23] is about 10% higher, that of Kempinnen[21] about 20% higher, and that of Sheppard[15] about 40% higher. The behavior of the present alloy does not seem to be much affected by the presence of the as-rolled substructure. It is known that a substructure created at one condition evolves to that of a new condition over strains of about 0.5.[4,8,9] The present peak strains at 10 s^{-1} are only slightly above those at 0.1 and 1.0 s^{-1}, possibly because it is easier to build up substructure density than to decrease it. The published reports do not give sufficient information on peak strains to make a comparison. The present values are only 10% higher than Q_{HW} for pure Al,[1,4,16,17,42] indicating that the DRV mechanisms are similar but more retarded at low T by dislocation interactions with particles and solute, which raise the strength considerably. Although n is low (1.9 to 1.27) in the sinh analysis, it is high ($>$4.9) in the power law; this leads to the conclusion that climb control is operative above the solute drag glide control domain.[1,4,45–48]

The strengths of the present alloy are consistent with those observed by Blum and co-workers[45–48] and McQueen and Belling[49] in Al, Al-4.8Mg, and Al-4.9Mg-0.6Mn (5083) with

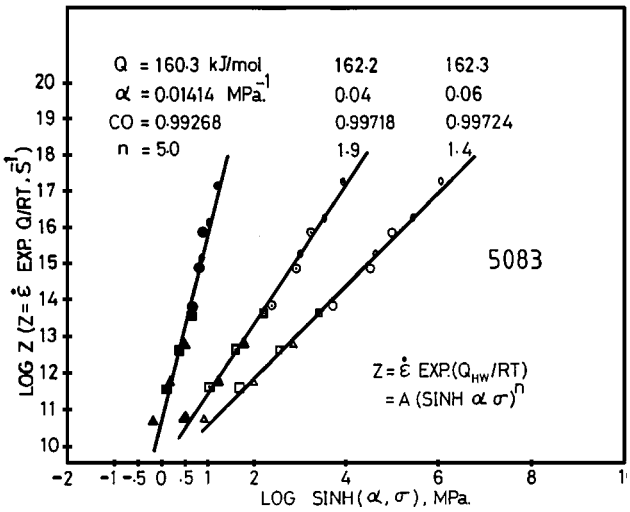

Fig. 8 The values of *Z*, which are calculated from the derived Q_{HW} and plotted against log sinh $\alpha\sigma$, result in a line confirming the validity of Eq 5. The lines have lower slopes (Å$n\alpha_v$) and move to higher values of sinh $\alpha\sigma$ as α increases. The fit is superior for the two lines α = 0.04 and 0.06 MPa^{-1}

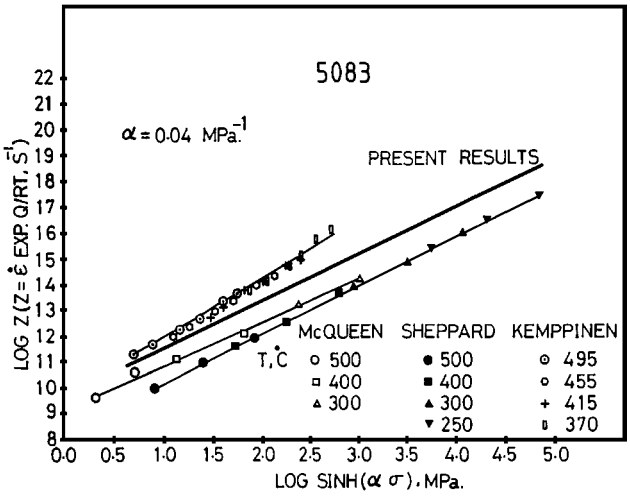

Fig. 9 Plots of log *Z vs* log sinh $\alpha\sigma$ with α = 0.04 MPa^{-1} provide comparison with other results, namely, McQueen and co-workers,[22,23] Sheppard,[14,15] and Kempinnen,[21] which have been recalculated for α = 0.04 MPa^{-1}. The present results are in the middle of a narrow band outlined by published data

the same impurities (0.03Fe, 0.02Si, and <0.01Ti) (at 500 °C, 0.1 s^{-1}: 9, 36, and 37 MPa, respectively, to 40 MPa presently); as *T* declines, the strengthening increases more rapidly in the same order (at 300 °C, 0.1 s^{-1}: 40, 170, and 180 MPa, respectively, to 160 MPa presently). The results of hot torsion tests to ε = 4 over the ranges 200 to 500 °C and 10^{-3} to 4 s^{-1} were compared to compression and tension creep results for minimum $\dot{\varepsilon}$ (ε < 2) in power-law plots, which showed good correspondence with curves varying in slopes at low σ from ~4.5 for Al and 5083 to ~3 for Al-5Mg with much higher values at high σ. The results were also plotted on a normalized basis ($\dot{\varepsilon}T/DG\mathbf{b}$) against ($\sigma$/G), where k is the Boltzman constant, *D* the diffusion coefficient (145 kJ/mol), **b** the Burgers vector, and *G* the shear modulus. The strength of 5083 was similar to Al-4.8Mg at medium stresses with a slope of 3, both being about 4 times stronger than Al, which had a slope of about 5. However, at low stresses, the 5083 diverged to higher strength than the Al-5Mg because of the strengthening by the dispersoid. The use of the common diffusion coefficient for Al or Mg atoms in Al alloys is clearly satisfactory for the creep regime (where there is good agreement with the 5083 behavior observed by Nakayama *et al.*[60]) but causes dispersion of the data points at high stresses. Hot tensile tests of 5083 ($\dot{\varepsilon}$ = 10^{-4} to 10^{-2} s^{-1}) were consistent in strength with the present tests and were fitted to the power law with 145 kJ/mole.[61]

5. Conclusions

As the temperature rises and the strain rate declines, the peak flow stress decreases and ductility increases so that the work softening and steady-stage regime become more noticeable. The exponential constitutive equation (β = 0.08 MPa^{-1}) proves suitable at these high stresses, but the power law is completely broken down. The hyperbolic sine function was found to be especially effective when α had values between 0.04 and 0.06 MPa^{-1} because of the following: (1) the *n* stress exponent is almost stable (1.9 to 1.3) and varies little with temperature; (2) the *S* temperature dependence increases linearly and varies little with strain rate; and (3) the activation energy Q_{HW} is constant (below α = 0.2, *n* and Q_{HW} vary rapidly, with an *n* of 5.0). In this range of α, $\beta = \alpha n$, and Q_{HW} has a value of 162 kJ/mol for both exponential and hyperbolic functions. Data sets from published literature also conformed closely with the above sinh analysis, with *n* varying through 1.73, 1.82, and 2.26 and Q_{HW} through 156, 162, and 185 kJ/mol, even though the strengths varied from +10 to +40% compared to the present alloy.

References

1. H.J. McQueen and M.E. Kassner: in *Superplasticity in Aerospace II*, T.R. McNelley, ed., TMS-AIME, Warrendale, PA, 1990, pp. 189-206.
2. H.J. McQueen and J.J. Jonas: *2nd Int. Conf. Properties of Al Alloys*, C.Q. Chen, ed., Beijing, 1990, pp. 727-42.
3. H.J. McQueen, E. Evangelista, and M.E. Kassner: *Z. Metallkd.*, 1991, vol. 82, pp. 336-45.
4. H.J. McQueen: in *Hot Deformation of Aluminum Alloys*, T.G. Langdon, and H.D. Merchant, eds., TMS-AIME, Warrendale, PA. 1991, pp. 31-54.
5. H.J. McQueen and O.C. Celliers: *Can. Metall. Q.*, 1996, vol. 35, pp. 303-19.
6. M.E. Kassner: in *Hot Workability of Steels and Light Alloys-Composites*, H.J. McQueen, E.V. Konopleva, and N.D. Ryan, eds., TMS-CIM, Montreal, 1996, pp. 217-26.
7. *Metals Handbook*, 10th ed., ASM International, Materials Park, OH, 1990, vol. 2, pp. 116-22.
8. H.J. McQueen: in *Hot Deformation of Al Alloys II*, T.R. Bieler, S. MacEwen, and L. Lalhi, eds., TMS-AIME, Warrendale, PA, 1998, pp. 383-96.
9. I. Poschmann and H.J. McQueen: *Z. Metallkd.*, 1997, vol. 88, pp. 14-22.
10. H.J. McQueen and I. Poschmann: in *THERMEC '97*, Woolongong, Australia, T. Chandra, ed., TMS-AIME, Warrendale, PA, 1997, pp. 951-57.

11. J.R. Pickens, W. Precht, and J.J. Mills: *Hot Rolling Simulation by Torsion of EMC and DC 5182,* Martin Marietta Labs, Baltimore, MD, 1984.
12. W. Precht and J.R. Pickens: *Metall. Trans. A,* 1987, vol. 18A, pp. 1603-11.
13. M. Ueki, S. Horie, and T. Nakamura: *J. Mech. Working Technol.,* 1985, vol. 11, pp. 365-76.
14. T. Sheppard: *Metall. Technol.,* 1981, vol. 8, pp. 130-41.
15. T. Sheppard: *Proc. 8th Light Metal Congr.,* J. Jeglitsch *et al.,* eds, The University of Leoben, Leoben, Austria, 1987, pp. 301-11.
16. H.J. McQueen and N. Ryum: *Scand. J. Metall.,* 1985, vol. 14, pp. 183-94.
17. H.J. McQueen and P. Sakaris: *Aluminum Alloys: Their Physical and Mechanical Properties—Proc. ICAA3,* L. Arnberg, E. Nes, O. Lohne, and N. Ryum, eds., NTH-Sinteff, Trondheim, Norway, 1992, vol. 2, pp. 179-84.
18. H.J. McQueen and J. Belling: in *THERMEC '97,* Woolongong, Australia, T. Chandra, ed., TMS-AIME, Warrendale, PA, 1997, vol. 1, pp. 965-71.
19. T. Sheppard and M.G. Tutcher: *Met. Sci.,* 1980, vol. 14, pp. 579-89.
20. T. Sheppard and M.G. Tutcher: *Met. Technol.,* 1981, vol. 8, pp. 319-27.
21. A.I. Kemppinen: *Deformation under Hot Working Conditions SP108,* Iron and Steel Institute, London, 1968, pp. 117-21.
22. H.J. McQueen, E. Evangelista, J. Bowles, and G. Crawford: *Met. Sci.,* 1984, vol. 18, pp. 395-402.
23. E. Evangelista, H.J. McQueen, and E. Bonetti: in *Deformation of Multi-Phase and Particle Containing Materials,* J. Bilde-Sorenson *et al.,* eds., Riso National Lab., Roskilde, Denmark, 1983, pp. 243-50.
24. H.J. McQueen and J.J. Jonas: *J. Appl. Metal Working,* 1984-85, vol. 3, pp. 233-41 and pp. 410-20.
25. H.J. McQueen and D.L. Bourell: *J. Met.,* 1987, vol. 39 (7), pp. 28-35.
26. H.J. McQueen: *Mater. Sci. Eng.,* 1987, vol. A101, pp. 149-60.
27. H.J. McQueen, E. Evangelista, and N.D. Ryan: in *Recrystallization ('90) in Metals and Materials,* T. Chandra, ed., TMS-AIME, Warrendale, PA, 1990, pp. 89-100.
28. T. Sheppard, M.A. Zaidi, M.G. Tutcher, and N.C. Parson: *in Microstructural Control in Al Alloy Processing,* H. Chia and H.J. McQueen, eds., TMS-AIME, Warrendale, PA, 1985, pp. 19-43, 123-54, and 155-78.
29. N. Raghunathan, H.B. McShane, C.P. Lee, and T. Sheppard: *Hot Deformation of Aluminum Alloys,* T.G. Langdon *et al.,* eds., TMS-AIME, Warrendale, PA, 1991, pp. 389-416.
30. K.G. Gardiner and R. Grimes: *Met. Sci.,* 1979, vol. 13, pp. 216-22.
31. T. Sheppard, M.G. Tutcher, and H.M. Flower: *Met. Sci.,* 1979, vol. 13, pp. 473-81.
32. J.J. Urcola and C.M. Sellars: *Acta Metall.,* 1987, vol. 35, pp. 2637-69.
33. M.R. Drury and F.J. Humphreys: *Acta Metall.,* 1986, vol. 34, pp. 2259-71.
34. H.J. McQueen, H. Chia and E.A. Starke: in *Microstructural Control in Al Alloy Processing,* H. Chia and H.J. McQueen, eds, TMS-AIME, Warrendale, PA, 1985, pp. 1-18.
35. F.J. Humphreys: *Acta Metall.,* 1977, vol. 25, pp. 1323-44.
36. F.J. Humphreys and P. Kalu: *Acta Metall.,* 1987, vol. 35, pp. 2815-29.
37. F.R. Castro-Fernandez and C.M. Sellars: *Met. Sci. Technol.,* 1988, vol. 4, pp. 621-27.
38. J.M. Belling, H.J. McQueen, B. Crawford, and A.S. Malin: in *Recrystallization '90,* T. Chandra, ed., TMS-AIME, Warrendale, PA, 1990, pp. 655-60.
39. J.R. Cotner and W.J. McG. Tegart: *J. Inst. Met.,* 1969, vol. 97, pp. 73-79.
40. M. Ueki, S. Horie, and T. Nakamura: in *Aluminum Alloys Physical and Mechanical Properties,* E.A. Starke and T.H. Sanders, eds., EMAS, Warley, United Kingdom, 1986, pp. 419-22.
41. H. Weiss, D.H. Skinner, and J.R. Everett: *J. Phys. E (Sci. Instrum.),* 1973, vol. 6, pp. 709-14.
42. W.A. Wong and J.J. Jonas: *Trans. TMS-AIME,* 1968, vol. 242, pp. 2271-80.
43. M.A. Wells, R. Bolingbroke, I.V. Samarasekera, E.B. Hawbolt, and J.K. Brimacombe: in *Light Metals Processing and Applications,* C. Bickert, M. Bouchard, G. Davies, E. Ghali, and E. Jiran, eds., TMS-CIM, Montreal, 1993, pp. 483-94.
44. E. Cerri, E. Evangelista, and H.J. McQueen: *High Temp. Mater. Proc.,* 1999, vol. 18, pp. 227-40.
45. W. Blum, Q. Zhu, R. Merkel, and H.J. McQueen (ICAA5): *Mater. Sci. Forum,* 1996, vol. 217–222, pp. 611-16.
46. W. Blum, Q. Zhu, R. Merkel, and H.J. McQueen: *Mater. Sci. Eng.,* 1996, vol. A205, pp. 23-30.
47. W. Blum, Q. Zhu, R. Merkel, and H.J. McQueen: *Z. Metallkd.,* 1996, vol. 87, pp. 14-23.
48. H.J. McQueen, W. Blum, Q. Zhu, and V. Demuth: in *Advances in Hot Deformation, Textures and Microstructures,* J.J. Jonas, T.R. Bieler, and K.J. Bowman, eds., TMS-AIME, Warrendale, PA. 1994, pp. 235-50.
49. H.J. McQueen and J. Belling: *Can. Met. Q.,* 2000, vol. 39, pp. 483-92.
50. D.M.R. Taplin and R.F. Smith: *in Fracture 1977 (ICF4),* D.M.R. Taplin, ed., University of Waterloo, Waterloo, 1977, pp. 541-51.
51. M. Otsuka and R. Horiuchi: in *Creep and Fracture of Engineering Materials and Structures,* B. Wilshire and D.R.J. Owens, eds., Pineridge Press, Swansea, United Kingdom, 1984, pp. 157-68.
52. D.J. Lloyd: *Metall. Trans. A,* 1980, vol. 11A, pp. 1287-94.
53. D.L. Yaney, J.C. Gibeling, and W.D. Nix: in *Strength of Metals and Alloys, ICSMA 7,* H.J. McQueen, J.-P. Bailon, J.I. Dickson, J.J. Jonas, and M.G. Akben, eds., Pergamon Press, Oxford, United Kingdom, 1986, vol. 2, pp. 887-92.
54. H.J. McQueen, W. Blum, and Q. Zhu: *in Superplasticity in Advanced Materials,* ICSAM '94, Moscow, T.G. Langdon, ed., Trans Tech Publications, Aedermannsdorf, Switzerland, 1994, pp. 193-200.
55. K. Matsuki, Y. Uetani, M. Yamada, and Y. Murakami: *Met. Sci.,* 1976, vol. 10, pp. 235-42.
56. E.M. Taleff, D.R. Lesuer, and J. Wadsworth: *Metall. Mater. Trans. A,* 1996, vol. 27A, pp. 343-52.
57. T. Sheppard, N.C. Parson, and M.A. Zaidi: *Met. Sci.,* 1983, vol. 71, pp. 481-90.
58. M.A. Zaidi and T. Sheppard: *Met. Sci.,* 1982, vol. 16, pp. 2229-38.
59. K. Lintermans and H.A. Kuhn: in *Aluminum Alloys—Physical and Mechanical Properties,* E.A. Stark and T.H. Sanders, eds., Engineering Materials Advisory Service, Warley, United Kingdom, 1987, pp. 529-43.
60. Y. Nakayama, K. Iwasaki, S. Goto, and H. Yoshinaga: *Trans. JIM,* 1990, vol. 31 p. 35.
61. E. Kovacs-Csetenyi, N.Q. Chin, and I. Kovacs (ICAA5): *Mater. Sci. Forum,* 1996, vol. 217-222, pp. 1175-80.